A combined crossed beam and *ab initio* investigation on the reaction of carbon species with C_4H_6 isomers. III. 1,2-butadiene, $H_2CCCH(CH_3)$ ($X\,^1A'$)—a non-Rice–Ramsperger–Kassel–Marcus system?

N. Balucani,[a)] H. Y. Lee,[b)] A. M. Mebel, Y. T. Lee, and R. I. Kaiser[c)]
Institute of Atomic and Molecular Sciences, 1, Section 4, Roosevelt Rd., 107 Taipei, Taiwan, Republic of China

Crossed molecular beam experiments were conducted to investigate the reaction of ground state carbon atoms, $C(^3P_j)$, with 1,2-butadiene, $H_2CCCH(CH_3)$ ($X\,^1A'$), at three collision energies of 20.4 kJ mol^{-1}, 37.9 kJ mol^{-1}, and 48.6 kJ mol^{-1}. *Ab initio* calculations together with our experimental data reveal that the reaction is initiated by a barrier-less addition of the carbon atom to the π system of the 1,2-butadiene molecule. Dominated by large impact parameters, $C(^3P_j)$ attacks preferentially the C2–C3 double bond to form **i1** (mechanism 1); to a minor extent, small impact parameters lead to an addition of atomic carbon to the C1–C2 bond yielding **i2** (mechanism 2). Both cyclic intermediates **i1** and **i2** ring open to triplet methylbutatriene complexes **i3'** ($H_2CC*CCH(CH_3)$) and **i3''**, ($H_2CCC*CH(CH_3)$); **C*** denotes the attacked carbon atom. **i3'** is suggested to decay nonstatistically prior to a complete energy randomization via atomic hydrogen loss forming 1- and 4-methylbutatrienyl CH_3CCCCH_2 ($X\,^2A''$) and $HCCCCH(CH_3)$ ($X\,^2A''$), respectively. The energy randomization in **i3''** is likely to be complete. This isomer decomposes via H atom loss to 3-vinylpropargyl, $H_2CCCC_2H_3(X\,^2A'')$, as well as 1- and 4-methylbutatrienyl radicals. In high-density environments such as the inner regions of circumstellar envelopes of carbon stars and combustion flames, these linear C_5H_5 isomers might undergo collision induced isomerization to cyclic structures like the cyclopentadienyl radical. This isomer is strongly believed to be a key intermediate involved in the production of polycyclic aromatic hydrocarbon molecules and soot formation. These characteristics make the reactions of atomic carbon with C_4H_6 isomers compelling candidates to form C_5H_5 isomers in the outflow of AGB stars and oxygen-deficient hydrocarbon flames. © *2001 American Institute of Physics.* [DOI: 10.1063/1.1385794]

I. INTRODUCTION

Experimental and theoretical investigations of the reactions of atomic carbon, $C(^3P)$, with C_4H_6 isomers are of great importance to understand the formation of various C_5H_5 isomers in extraterrestrial environments and sooting hydrocarbon flames. Elementary reactions of $C(^3P)$ with the two isomers 1,3-butadiene, $H_2CCHCHCH_2$,[1] and dimethylacetylene, H_3CCCCH_3,[2] have been recently studied to investigate potential formation routes of the cyclopentadienyl radical, c-C_5H_5, in oxygen-deficient hydrocarbon flames and carbon-rich outflows of late-type (AGB) carbon stars. An active role of c-C_5H_5 together with benzene has been invoked by chemical models to explain the formation of polycyclic aromatic hydrocarbons (PAH) in those environments,[3] but the route of formation of the radical itself has not been understood yet. Very recently, we verified that products of gross formula C_5H_5 are actually formed from the reactions of

atomic carbon with $H_2CCHCHCH_2$ and H_3CCCCH_3. However, the first reaction was observed to form predominantly the 1- and 3- vinylpropargyl radicals, $HCCCHC_2H_3$ ($X\,^2A''$), and $H_2CCCCC_2H_3$ ($X\,^2A''$), while the second leads predominantly to the 1-methylbutatrienyl radical, $H_2CCCCCH_3$ ($X\,^2A''$). Quite interestingly, the main products formed starting from the two different C_4H_6 isomers are distinct, which is a consequence of the site specificity of the $C(^3P)$ attack and the involved potential energy surfaces (PESs). In this paper, we report a combined experimental and theoretical investigation on the reaction of carbon atoms with the third C_4H_6 isomer, namely 1,2-butadiene. Similarities and differences with respect to the reactions with both 1,3-butadiene and dimethylacetylene will be noted, and the potential implication in combustion and interstellar chemistry will be assessed.

II. EXPERIMENTAL SETUP

The experiments were performed employing the 35″ crossed molecular beams machine described in details elsewhere,[4] and only a brief description is given here. A pulsed supersonic carbon beam was generated via laser ablation of graphite at 266 nm.[5] The 30 Hz, 35–40 mJ output of a Spectra Physics GCR-270-30 Nd:YAG laser was focused onto a rotating carbon rod, and the ablated species

TABLE I. Experimental beam conditions and 1σ errors averaged over the experimental time: peak velocity v_p, speed S, peak collision energy, E_{coll}, and the center-of-mass angle, $\Theta_{c.m.}$.

Beam	v_p, m s^{-1}	S	E_c, kJ mol^{-1}	$\Theta_{c.m.}$
$C(^3P_j)$	1890 ± 10	6.6 ± 0.3	20.4 ± 0.3	61.4 ± 0.2
$C(^3P_j)$	2670 ± 20	4.5 ± 0.2	37.9 ± 0.5	52.4 ± 0.2
$C(^3P_j)$	3050 ± 20	4.8 ± 0.2	48.6 ± 0.6	49.0 ± 0.4
C_4H_6	770 ± 10	8.0 ± 0.1		

were seeded into a pulse of neat helium gas. A four-slot chopper wheel mounted after the ablation zone selected a 9.0 μs segment of the seeded carbon beam, cf. Table I. The carbon beam crossed a pulsed pure 1,2-butadiene beam at 90° in a large scattering chamber kept at a pressure in the range of 10^{-7} mbar. The scattered reaction products were detected in the plane defined by the two beams using a rotating detector, which consists of a Brink-type electron-impact ionizer,[6] a quadrupole mass filter, and a Daly ion detector. The velocity distribution of the products was recorded using the time-of-flight (TOF) technique (typical accumulation time up to 60 min) at distinct laboratory angles. Information on the reaction dynamics was gained by fitting the TOF spectra and the product angular distribution in the laboratory frame (LAB) by means of a forward-convolution routine of trial center-of-mass (c.m.) angular, $T(\theta)$, and product translational energy, $P(E_T)$, distributions.[7] The LAB TOF and angular distributions are iteratively calculated from trial $T(\theta)$ and $P(E_T)$ and averaged over the apparatus and beam functions, until the best fit of LAB distributions is achieved. The final outcome of this kind of procedure is the generation of a product flux contour map, which reports the differential cross section as a function of the c.m. scattering angle, θ, and c.m. product velocity, u, that $I(\theta,u)=P(u) \times T(\theta)$.

III. *AB INITIO* AND RICE–RAMSPERGER–KASSEL–MARCUS CALCULATIONS

Geometries of the reactants, final products, intermediates, and transition states for the reaction of atomic carbon in its ^3P_j electronic ground state with 1,2-butadiene were optimized using the hybrid density functional B3LYP method, i.e., Becke's three-parameter nonlocal exchange functional[8] with the nonlocal correlation functional of Lee, Yang, and Parr[9] and the 6-311G(d, p) basis set.[10] Vibrational frequencies, calculated at the B3LYP/6-311G(d, p) level, were used for characterization of stationary points and zero-point energy (ZPE) correction. All the stationary points were positively identified for minimum or transition state. In some cases, geometries and frequencies were recalculated at the MP2/6-311G(d, p) and CCSD(T)/6-311G(d, p) level.[11] The GAUSSIAN 94,[12] MOLPRO 96,[13] and ACES-II[14] programs were employed for the potential energy surface computations. In addition to *ab initio* electronic structure calculations, we performed Rice–Ramsperger–Kassel–Marcus (RRKM) theory[15] calculations to derive the different rate constants $k(E)$ of individual reaction steps for the unimo-
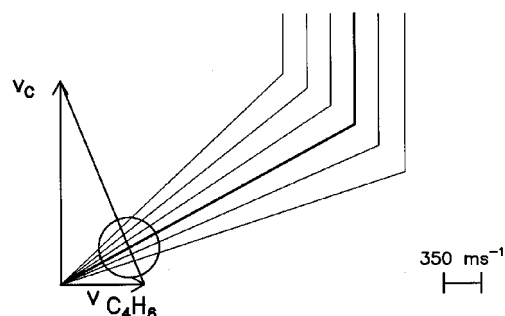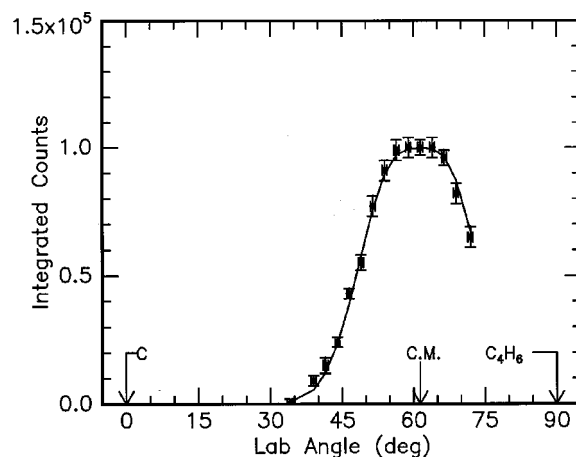

FIG. 1. Lower: Newton diagram for the reaction $C(^3P_j)$ $+H_2CCCH(CH_3)(X\,^1A')$ at a collision energy of 20.4 kJ mol^{-1}. Upper: Laboratory angular distribution of product channel at $m/e=63$. Circles and 1σ error bars indicate experimental data, the solid lines the calculated distribution. c.m. designates the center-of-mass position angle. The solid lines originating from the Newton diagram point to distinct laboratory angles whose TOFs are shown in Fig. 4.

lecular reaction $A^* \to A^\# \to P$ where $A^\#$ is the activated complex, A^* is the energized reactant molecule, and P are the possible products.[1]

IV. RESULTS

A. Reactive scattering signal and TOF spectra

At the three collision energies investigated, we have detected reactive scattering signal at mass to charge ratios, m/e, starting from 65 to 60, corresponding to the ions $C_5H_5^+$ to C_5^+ (Figs. 1–6). No radiative association to $C_5H_6(m/e=66)$ was found. Since the TOF spectra recorded at different m/e values could be fit with the same c.m. functions, we can conclude that the signal at m/e ratios lower than the highest one (65) actually originates from dissociative ionization of C_5H_5 in the ionizer. Therefore, we can exclude that the H_2 elimination channel is open under our experimental conditions. The detection of a possible methyl group elimination pathway suffers leading to H_3+CH_3 suffers from the inherent high background levels present at mass to charge ratios from 51 ($C_4H_3^+$) to 48(C_4^+) due to ionization—fragmentation of the 1,2-butadiene in the ionizer.
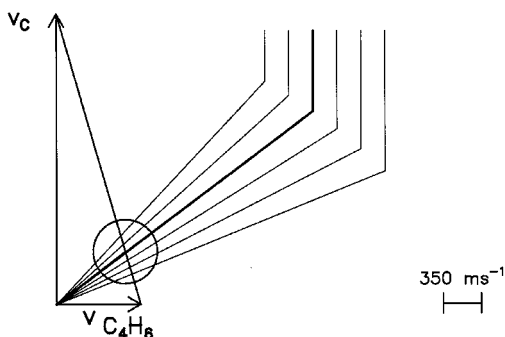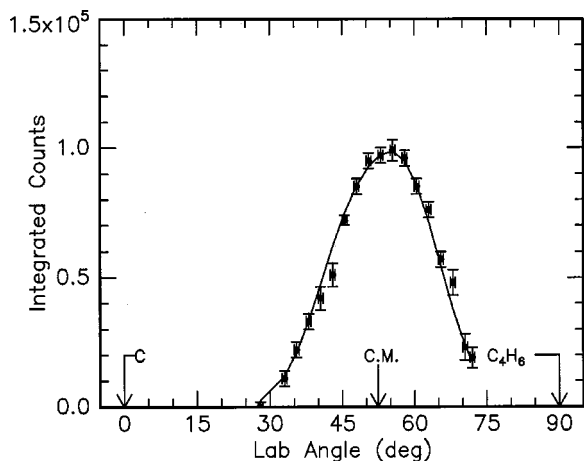
J. Chem. Phys., Vol. 115, No. 11, 15 September 2001

Reaction of carbon species with C_4H_6. III   5109

FIG. 2. Lower: Newton diagram for the reaction $C(^3P_j)$ $+H_2CCCH(CH_3)(X\,^1A')$ at a collision energy of 37.9 kJ mol^{-1}. Upperer: Laboratory angular distribution of product channel at $m/e=63$. Circles and 1σ error bars indicate experimental data, the solid lines the calculated distribution. c.m. designates the center-of-mass angle. The solid lines originating from the Newton diagram point to distinct laboratory angles whose TOFs are shown in Fig. 5.

FIG. 3. Lower: Newton diagram for the reaction $C(^3P_j)$ $+H_2CCCH(CH_3)(X\,^1A')$ at a collision energy of 48.6 kJ mol^{-1}. Upper: Laboratory angular distribution of product channel at $m/e=63$. Circles and 1σ error bars indicate experimental data, the solid lines the calculated distribution. c.m. designates the center-of-mass angle. The solid lines originating from the Newton diagram point to distinct laboratory angles whose TOFs are shown in Fig. 6.

B. Laboratory angular distributions

The most probable Newton diagrams of the reaction of atomic carbon with 1,2-butadiene together with the measured laboratory angular distributions are displayed in Figs. 1–3. The whole set of data was taken at $m/e=63$ since this mass-to-charge ratio was characterized by the best signal-to-noise ratio. All LAB angular distributions are very broad and extend up to 55.0 ° in the scattering plane defined by the two intersecting beams. At the lowest collision energy of 20.4 kJ mol^{-1}, the LAB angular distribution peaks close to $\Theta_{c.m.}$ (the c.m. velocity vector angle) and shows intensity both at the right and the left of $\Theta_{c.m.}$, suggesting that the reaction which forms C_5H_5 and atomic hydrogen proceeds via indirect reactive scattering dynamics, that is through the formation of C_5H_6 complex(es). Notice also that the TOF spectra recorded at $\Theta=56.5°$ and $61.5°$ depict pronounced shoulders. With the increase of collision energy, the LAB angular distributions become more asymmetric and peak in the backward direction, relatively to the initial direction of the atomic carbon beam.

C. Center-of-mass translational energy distributions, $P(E_T)$

The best-fit translational energy distributions are shown in Figs. 7–9 with the relative error bounds. At each collision
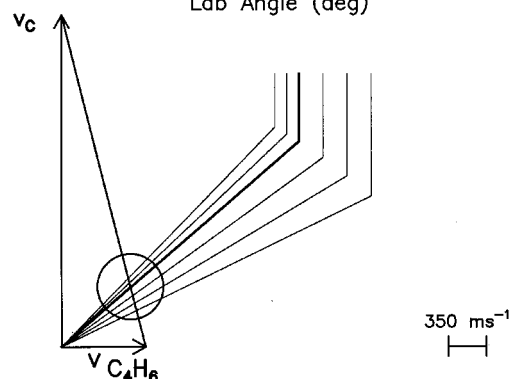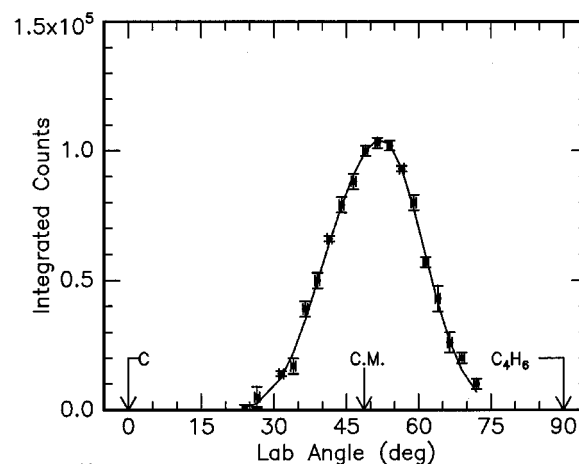
energy, both the TOF and angular distributions could be fitted using a single $P(E_T)$ for the whole range of scattering angles. The $P(E_T)$ distributions stretch out to maximum translational energies, E_{max}, between 180 and 240 kJ mol^{-1}. The addition of a long tail up to 300–310 kJ mol^{-1} with an intensity of 0.02–0.03 [relatively to the peaks of each $P(E_T)$] does not change the quality of the fit significantly. Whenever the thermochemistry of the channels leading to distinct product isomers is very different, the maximum value reached by the product translational energy (which cannot exceed the sum of the reaction exothermicity and the relative collision energy) can unravel the nature of the reaction product(s). If we account for the relative collision energies, the experimentally derived heat of reaction is about 190 ± 20 kJ mol^{-1}. If we consider also the long energy tail, the formation of some product isomers might be an exothermic as 270 kJ mol^{-1}. Another interesting characteristic of the best-fit $P(E_T)$s is the peak position which is at about 35–45 kJ mol^{-1} in all cases, that is well away from zero translational energy; this experimental finding suggests that the reaction might have a tight exit transition state.

D. Center-of-mass angular distributions, $T(\theta)$, and product flux contour maps $I(u,\theta)$

At the lowest collision energy, the best-fit $T(\theta)$ and the relative $I(\theta,u)$ are symmetric around $\pi/2$ and show constant
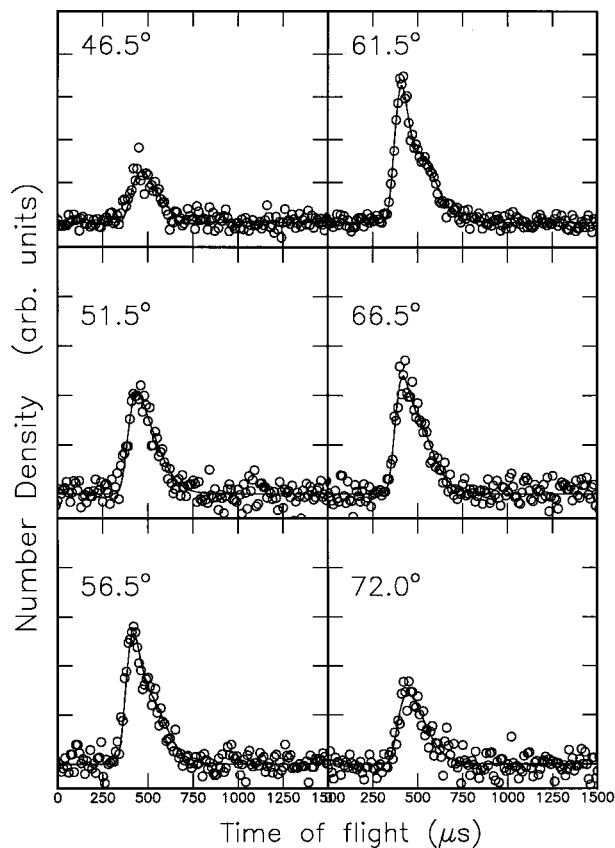
FIG. 4. Time-of-flight data at $m/e = 63$ for indicated laboratory angles at a collision energy of 20.4 kJ mol^{-1}. Open circles represent experimental data, the solid lines are the calculated curves when using the c.m. best-fit functions.

FIG. 5. Time-of-flight data at $m/e = 63$ for indicated laboratory angles at a collision energy of 37.9 kJ mol^{-1}. Open circles represent experimental data, the solid lines are the calculated curves when using the c.m. best-fit functions.

intensity in the whole angular range (they are perfectly isotropic, as well visible in Figs. 7 and 10). A slightly sideways peaking of $T(\theta)$ [up to $T(0°)/T(90°) = 0.92$] gives a good fit of the data as well. One possible explanation for the symmetry of the angular distribution can be given if we assume that the reaction proceeds via indirect scattering dynamics through the formation of C_5H_6 complex(es), the lifetime(s) of which is(are) longer than the rotational period, τ_r. The weak polarized angular distribution is likely the effect of the poor coupling between the initial and final angular momentum vectors, $\mathbf{L}$ and $\mathbf{L}'$, respectively, which is a consequence of the light H atom emission. In fact, since total angular momentum $\mathbf{J}$ must be conserved, a large fraction of the initial orbital angular momentum has to be channeled into rotational excitation of the C_5H_5 product, that is the initial angular momentum is mainly converted into C_5H_5 rotational momentum.

Another possible explanation is that the geometry of the collision intermediate is such that two hydrogen atoms can be interconverted through a rotational axis.[16] In this case, the light H-atom could be emitted along a direction defined by θ and $\theta-\pi$ with the same probability and the result is the forward–backward symmetry of $T(\theta)$.

One last possibility is that the observed isotropic distribution is actually originated by the superposition of the contributions of different direct reactions; in this case the experimental findings is the result of the averaging over a
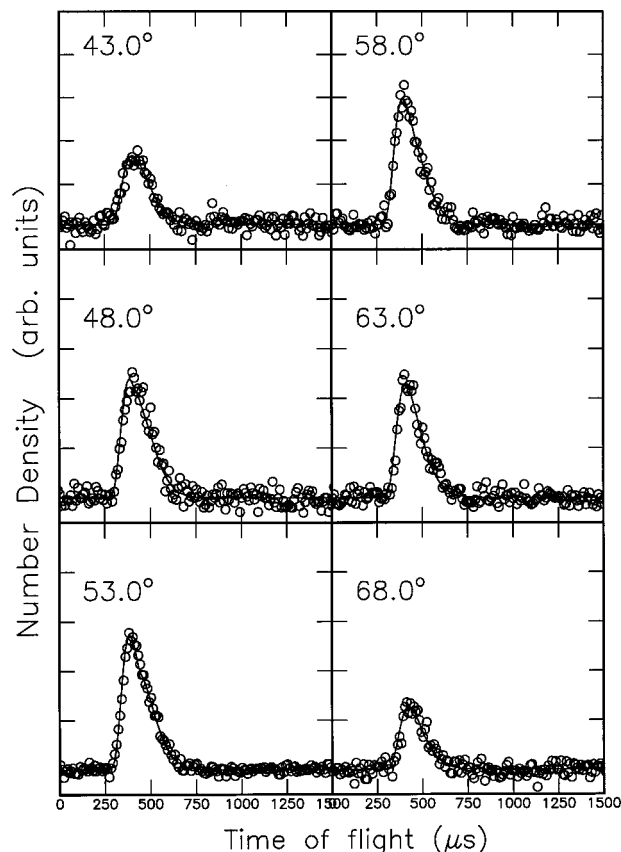
distribution of active impact parameters. In this assumption, small impact parameters generates backward scattered products, large impact parameters generate forward scattered products, and medium impact parameters generate sideways scattered products; the observed isotropic distribution will be just the result of a compensation amongst the three types of contributions.

Quite interestingly, with the increase of the collision energy, the shape of the c.m. angular distributions and the flux contour maps changes significantly from a symmetric ($E_c = 20.4$ kJ mol^{-1}) to a backward biased distribution [$T(0°)/T(180°) = 0.69–0.74$ at $E_c = 37.9$ kJ mol^{-1} and $T(0°)/T(180°) = 0.52–0.54$ at $E_c = 48.6$ kJ mol^{-1}] cf. Figs. 7–10. This trend can be accounted for by different scenarios. One possibility is that the reaction dynamics involve only one microchannel which is the one previously suggested occurring through the formation of a complex; the decomposing complex would be long lived at low, but short lived at high collision energies. A second possibility is that two distinct microchannels are involved: a long-lived intermediate at all collision energies (microchannel 1) plus a second fragmenting complex which is long lived at low, but short lived at both high collision energies (microchannel 2). If we resort to the assumption that the symmetric $T(\theta)$ at the low collision energy is generated by a distribution of impact parameters, the preference for backward scattering observed in the
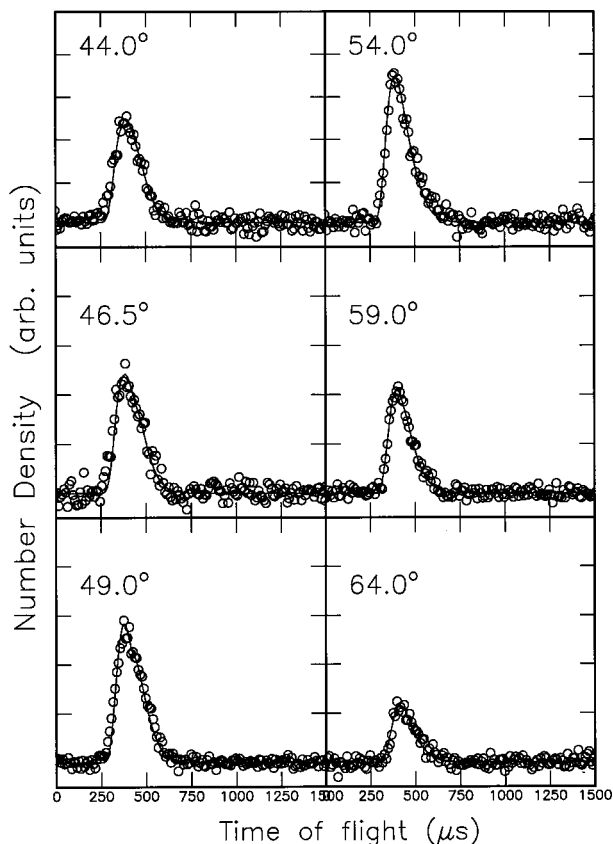
J. Chem. Phys., Vol. 115, No. 11, 15 September 2001

Reaction of carbon species with C_4H_6. III   5111

FIG. 6. Time-of-flight data at $m/e = 63$ for indicated laboratory angles at a collision energy of 48.6 kJ mol^{-1}. Open circles represent experimental data, the solid lines are the calculated curves when using the c.m. best-fit functions.

high energy experiments can be attributed to the quenching of the large impact parameters with the increase of the collision energy.

V. DISCUSSION

A. The C_5H_6 potential energy surface

Despite an extensive exploration, no transition states for a $C(^3P_j)$ insertion into C–H and the C–C bonds of 1,2-butadiene could be located. The carbon atom was found to add to the olefinic bonds of 1,2-butadiene without entrance barrier, Fig. 11. Since the C1–C2 and C2–C3 double bonds are not identical, two initial collision complexes could be formed. An attack to C2/C3 yields a tricyclic intermediate **i1**, whereas interaction with C1/C2 forms **i2**. Upon addition, the adjacent carbon–carbon double bonds elongate from 130.4 pm to 135.7 pm (**i1**) and 135.4 pm (**i2**) slightly longer than the ethylenic carbon–carbon bond length of 134 pm. Both intermediates reside in a potential energy well, are stabilized by 275.9 and 280.9 kJ mol^{-1}, and can isomerize to each other through a transition state located 199.9 kJ mol^{-1} below the separated reactants. As the C1–C2 and C2–C3 bonds are very long (161.7 pm and 161.0 pm), a common pathway of **i1** and **i2** is a ring opening via low barriers of 41 kJ mol^{-1} and 48 kJ mol^{-1}, respectively, to give a triplet methylbutatriene radical **i3** which is the global energy minimum of this part of the PES (-430.4 kJ mol^{-1}). In strong contrast to

the $C(^3P_j)/H_2CCCH_2$ system, no local minimum corresponding to the initial addition to the central carbon atom C2 of the 1,2-butadiene molecule could be located. This structure was found to be rather a first order saddle point of the **i1**↔**i2** isomerization, cf. Fig. 12. Since the barriers of hydrogen shifts in **i1** and **i2** are in the order of 150–200 kJ mol^{-1},[17] these pathways cannot compete with the ring

FIG. 7. Center-of-mass translational energy flux distribution (upper) and center-of-mass angular distribution (lower) for the reaction $C(^3P_j)$ $+ H_2CCCH(CH_3)(X\,^1A') \rightarrow C_5H_5 + H$ at collision energy of 20.4 kJ mol^{-1}.

FIG. 8. Center-of-mass translational energy flux distribution (upper) and center-of-mass angular distribution (lower) for the reaction $C(^3P_j)$ $+ H_2CCCH(CH_3)(X\,^1A') \rightarrow C_5H_5 + H$ at collision energy of 37.9 kJ mol^{-1}.
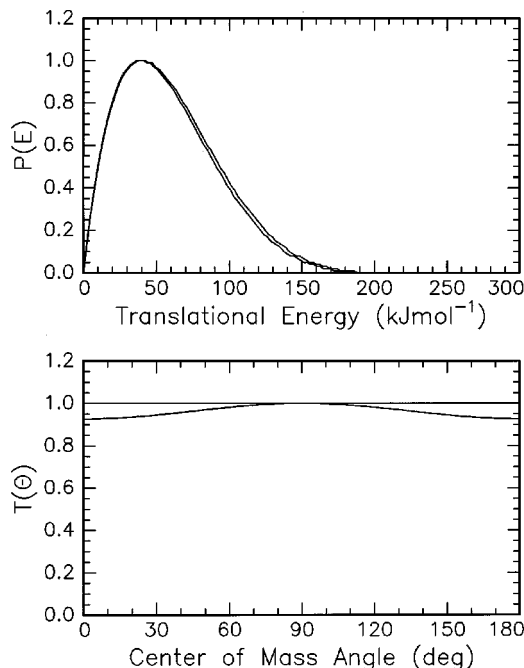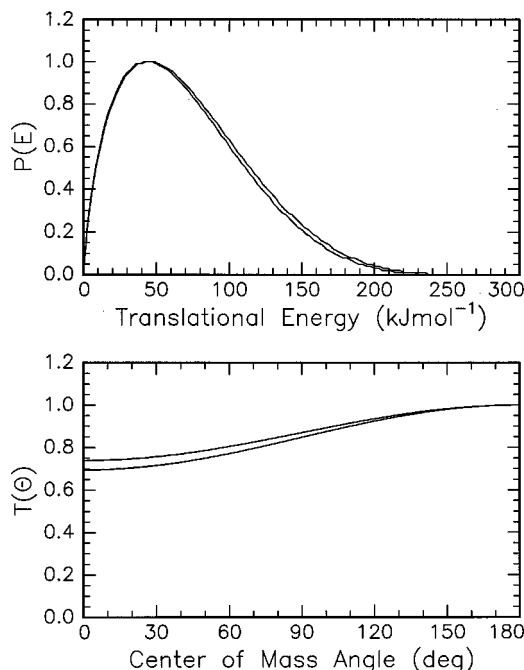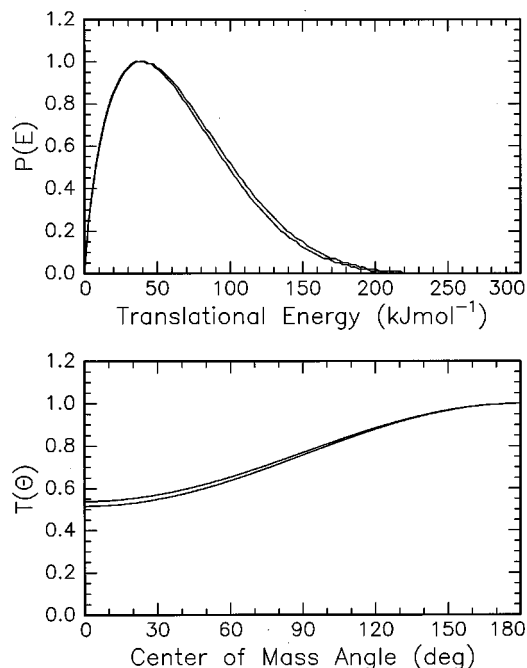
FIG. 9. Center-of-mass translational energy flux distribution (upper) and center-of-mass angular distribution (lower) for the reaction $C(^3P_j)$ $+H_2CCCH(CH_3)(X\,^1A')\rightarrow C_5H_5+H$ at collision energy of 48.6 kJ mol^{-1}.

opening process to **i3**. The latter can fragment via H atom elimination to 3-vinylpropargyl (**p4**) (C_s point group; $^2A''$ ground state), 1-methylbutatrienyl (**p2**)(C_s; $^2A''$), and/or 4-methylbutatrienyl (**p3**) (C_s point group; $^2A''$) via tight exit transition states located 13–24 kJ mol^{-1} above the separated products; in contrast to the n-C_4H_3 molecule which is bent,[18] both methyl substituted isomers **p2** were found to have linear butatrienyl like radical substructures. Finally, a potential methyl group loss channel from **i3** can lead to the n-C_4H_3 molecule.

B. Identification of the reaction product(s)

The translational energy distributions, $P(E_T)$s, show that the reaction leading to the C_5H_5 product(s) is exothertic by 190 ± 20 kJ mol^{-1}; the additional tail could account up to an exothermicity of 270 kJ mol^{-1}. If we compare these findings with our electronic structure calculations, it is evident that the energetically more favorable C_5H_5 isomer **p4** can only be a minor reaction product under the present experimental conditions. The computed reaction enthalpy of this channel is -259.8 kJ mol^{-1} and is in good agreement with previous experimental data. Based on the energetics, our results rather suggest the formation of **p2** and/or **p3**. In fact, these reaction channels were found to be exothermic by 189.0 and 177.3 kJ mol^{-1} and these values are in good agreement with that (190 ± 20 kJ mol^{-1}) determined from c.m. translational energy distributions. Interestingly, the conclusion that **p2** and/or **p3** are the main reaction products is in strong disagreement with microcanonical transition state calculations predicting branching ratios of 71.8:2.3:1.4:24.4 for the decomposition of **i3** into **p4**:**p3**:**p2**:**p1**. Therefore, the experimental findings suggest that the decomposition of **i3** is a nonstatistical process and that the intramolecular energy dis-
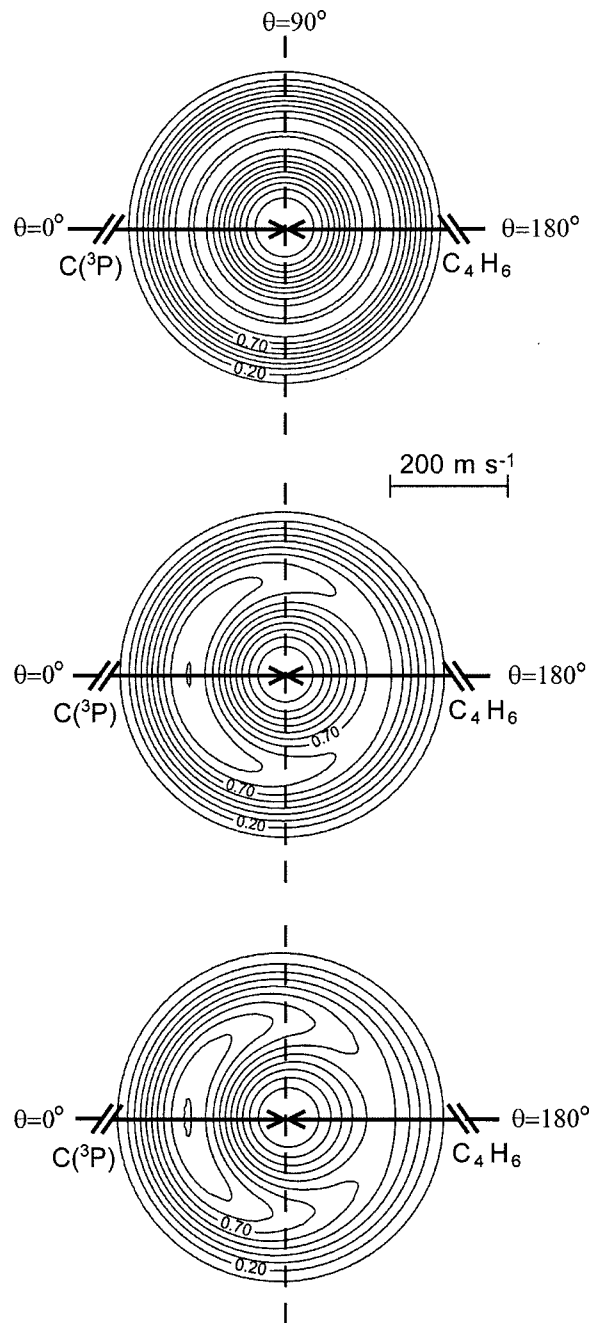
FIG. 10. Contour flux map for the reaction $C(^3P_j)$ $+H_2CCCH(CH_3)(X\,^1A')\rightarrow C_5H_5+H$ at a collision energy of 20.4 kJ mol^{-1}. (top), 37.9 kJ mol^{-1} (middle), and 48.6 kJ mol^{-1} (bottom).

ribution is not rapid on the time scale of the reaction. The nonstatistical behavior suggests that the energy may not become statistically redistributed in the range of time between the initial bond formation and the subsequent bond breaking, so that only distinct modes are activated. The lifetime of the complex is too short for a complete energy randomization to occur.[19]

C. The actual reaction pathway on the C_5H_6 potential energy surface

We now address the question: what are the underlying dynamics to form the C_5H_5 isomers **p1**, **p2**, and **p3**? Based

FIG. 11. Schematic representation of the lowest energy pathways on the triplet C_5H_6 PES of the $C(^3P_j)+H_2CCCH(CH_3)$ $(X\,^1A')$ reaction together with structures of potentially involved collision complexes, reactants, and products. Important bond lengths are given in Å, bond angles in degrees.

on our experimental data, the reaction dynamics are suggested to be indirect via the formation of a strongly bound intermediate. The singly occupied p_x and p_y orbitals of $C(^3P_j)$ interact with the π orbital at the carbon–carbon double bond to form **i1** and **i2** without any potential energy barrier, cf. Fig. 11. These pathways support maximum orbital overlaps to form two C–C–σ bonds in the cyclopropylidene substructure. Since the reaction has no entrance barrier and is
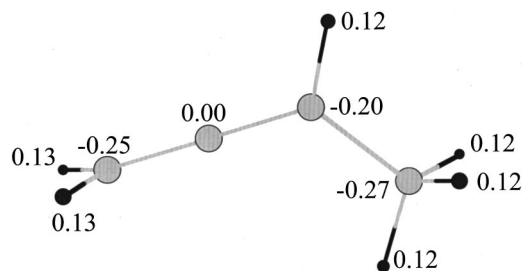

FIG. 12. Stationary point of the formal addition of $C(^3P_j)$ to the central carbon atom of 1,2-butadiene; the imaginary frequency of 301.85 cm^{-1} corresponds to the carbon–carbon bending mode leading to ring closure. Important bond lengths are given in Å, bond angles in degrees.

dominated by long range dispersion forces, predominantly large impact parameters are suggested to dictate the initial complex formation in a similar way as in the $C(^3P_j)$/allene system.[18] Therefore, reactions with large impact parameters likely dominate, and carbon atoms add preferentially to the C2–C3 double bond to form **i1** rather then interact with the C1–C2 bond to **i2**. Furthermore, the concept of regioselectivity of electrophilic attacks on unsaturated hydrocarbon molecules predicts that the addition is directed towards the bond which holds the highest negative charge at each atom. Since the π group orbitals of the methyl group enhance the spin density of the C3, an addition to the C3–C2 bond is preferred, cf. Fig. 13. Finally, the bulky methyl group reduces the cone of acceptance of the C1 atom thus directing the addition preferentially to form **i1**. Therefore, two micromechanisms are likely to control the formation of the initial addition complex: reactions with large impact parameter lead preferentially to intermediate **i1** (micromechanism 1) whereas—to a minor amount—trajectories with low impact parameters give **i2** (micromechanism 2). Since the total angular momentum **J** must be conserved, the initial angular momentum **L** leads to a rotational excitation of the final C_5H_5 isomer product(s). In this approximation we imply that the light hydrogen atom cannot carry away a significant

FIG. 13. Charge densities in the triplet methylbutatriene intermediate derived from the population analyses.

FIG. 14. Location of the center-of-mass and principal rotational axes in the decomposing complex **i3**.

amount of final angular momentum, and hence $\mathbf{J}=\mathbf{L}\approx\mathbf{j}'$ with $\mathbf{j}'$ representing the final rotational angular momentum. Therefore, the four carbon atoms are expected to rotate in a plane approximately perpendicular to $\mathbf{L}$ around the B/C axes of the intermediates. The consecutive ring opening conserves the rotational axes B/C of the highly prolate triplet methylbutatriene complex **i3**, $\kappa=-0.994$, cf. Fig. 14. Although both ring openings of **i1** and **i2** lead to methylbutatriene, the resulting complexes are not equivalent as the carbon atom is formally inserted between C2–C3(**i3'**) and C1–C2(**i3''**), cf. Fig. 15. We like to stress that although **i1** and **i2** are connected via a transition state (Fig. 11), this isomerization barrier is 35–37 kJ mol^{-1} larger than barriers of both ring opening. This significant energy difference very likely conserves the initial concentration of **i1** (large impact parameter reactions) versus **i2** (low impact parameter reactions). This impact parameter-dependent formation of two distinct triplet methylbutatriene complexes **i3'** and **i3''** holds the key for the nonstatistical behavior. The RRKM treatment assumes that upon formation of the new bond, the intramolecular energy distribution is rapid and the energy is completely randomized before the final carbon–hydrogen bond ruptures. Therefore, any RRKM-based investigation of the C($^{3}P_j$) reaction with 1,2-butadiene does not distinguish between **i3'** and **i3''** although they arise from distinct microchannels and hence different vibrational modes can be initially activated. Denoting

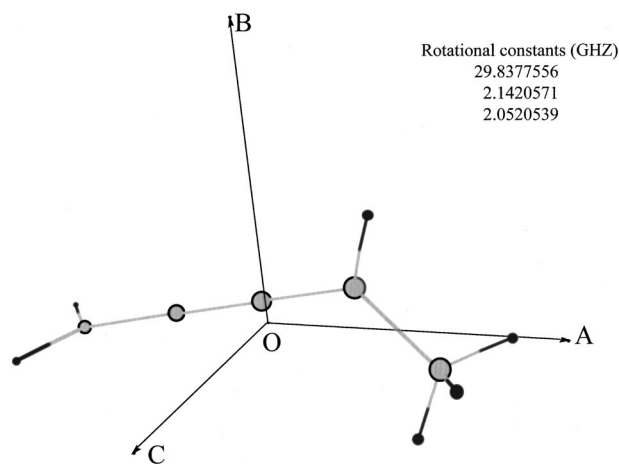the reactant carbon atom as $\mathbf{C}^*$, we expect an initial excitation of the $\mathbf{C}^*=$C2 and C3$=\mathbf{C}^*$ stretching modes in **i3'**, whereas the $\mathbf{C}^*=$C1 and C2$=\mathbf{C}^*$ vibrations should be excited initially in **i3''**. Consequently, the formation of the energetically most favorable 4-vinylpropargyl radical (**p4**) requires the energy to be transferred over four (**i3'**) and three (**i3''**) bonds from the initially activated bond to the carbon–hydrogen bond of the methyl group. Since **p4** is suggested to be only a minor product of the reaction which is itself dominated by small impact parameters to form **i1** and hence **i3'**, the energy randomization in **i3'** is likely not completed. Otherwise, if the energy were statistically distributed before the bond cleavage, we would expect a prevailing formation of **p4**. This suggests that **i3''** rather than **i3'** represents the decomposing complex to form **p4** plus atomic hydrogen. Additionally, since the absolute contribution of **p4** to the reactive scattering signal was suggested to be small, these findings verify that the reaction is dominated by large impact parameters and that the formation of **i3''** via microchannel 2 represent only a small fraction of the products. Therefore, rather
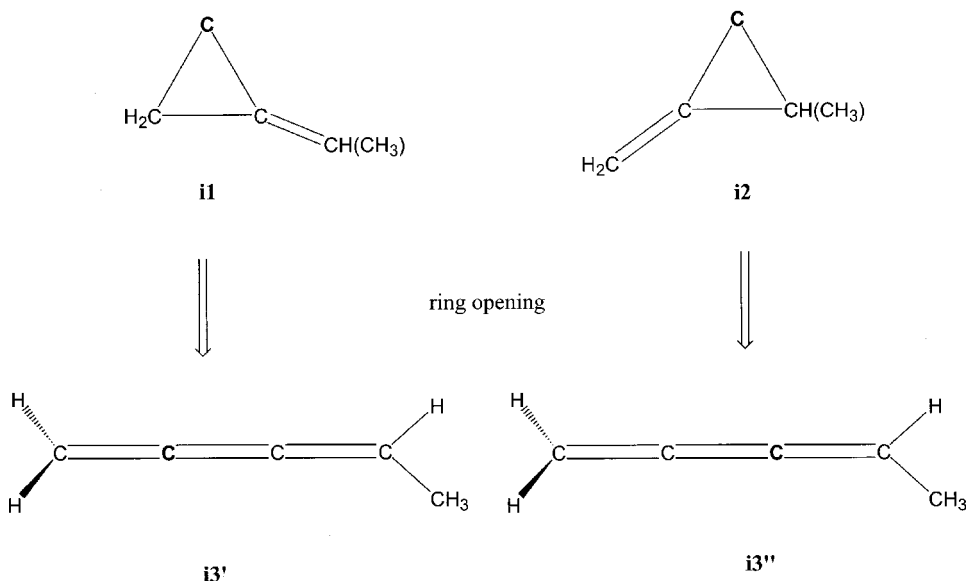

FIG. 15. Schematic representation of the ring opening of intermediates **i1** and **i2** to **i3'** (left) and **i3''** (right).
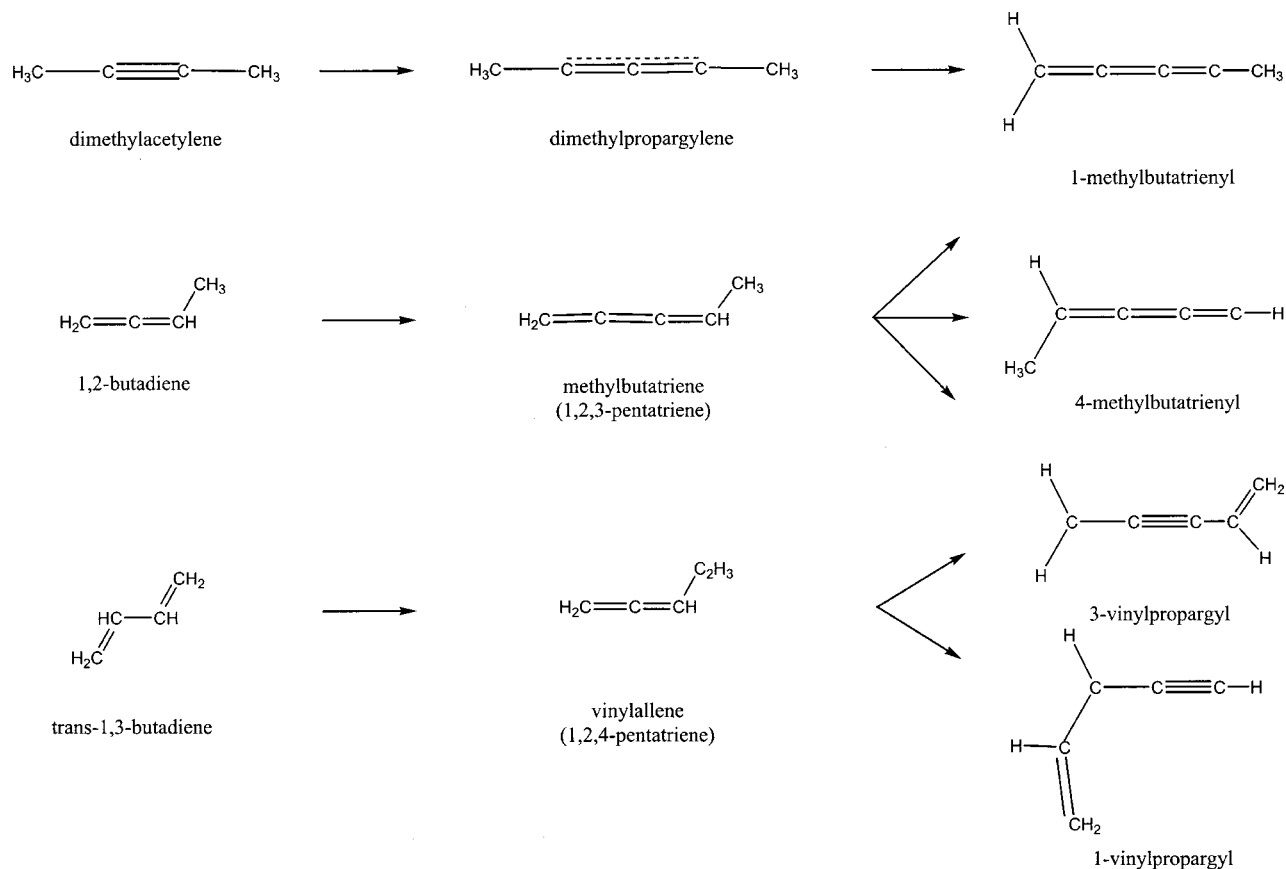
FIG. 16. Distinct decomposing complexes (center) and C$_5$H$_5$ isomers (right) formed upon reaction of atomic carbon with three different C$_4$H$_6$ isomers (left).

than decomposing to 3-vinylpropargyl, **i3′** fragments predominantly to **p2** and/or **p3** as proposed via our experimentally determined reaction exothermicity. These pathways require that the energy channels only into two (to the adjacent H–C3 bond forming **p3**) or three bonds to C1–H into the reaction coordinate, compared to four bonds necessary for the hydrogen loss of the methyl group. Likewise, **i3″** complexes are expected to react to **p2** and **p3**. At lower collision energy, the lifetime of the deomposing complexes are longer than their rotational periods which are in the order of 1 ps (forward–backward center-of-mass angular distribution), but suggested to be too short before a complete energy randomization occurs.

As we have seen, the nonstatistical behavior could be explained within the frame of a bound **i3′** intermediate. These patterns are similar to the classical non-RRKM behavior reported by Rynbrandt et al.[18,19] Here, singlet methylene reacted with hexafluorovinylcyclopropane to produce a bicyclic, chemically activated species via addition of methylene to the carbon–carbon double bond. Their bulk experiments result indicated that the energy flow between both cyclopropyl rings takes about 300 ps. If we infer single collision conditions, a hypothetical crossed beam experiment would depict a symmetric center-of-mass angular distribution at lower collision energies (lifetime of the decomposing complex larger than about 1 ps), but the energy randomization would be still incomplete. A similar case was found for chemically activated C$_2$H$_4$F complexes in the crossed beam study of the reaction of ethylene with fluorine atoms.[20]

There, the $T(\theta)$s were found to be forward–backward symmetric, but the experiments indicated a nonstatistical decay of the complex as well.

VI. CONCLUSIONS

The reaction of ground state carbon atoms, $C(^3P_j)$, with 1,2-butadiene was studied at three different collision energies of 20.4, 37.9, and 48.6 kJ mol^{-1} by employing the crossed molecular beam technique; the experimental results have been combined with electronic structure calculations. The reaction is initiated by a barrier-less interaction of the carbon atom with one of the two π bonds of the 1,2-butadiene molecule. In the light of electronic structure calculations, our experimental findings suggest that most likely $C(^3P_j)$ attacks preferentially the C2–C3 double bond with large impact parameters to form the intermediate **i1** (mechanism 1). To a minor extent, collisions with small impact parameters lead to the addition of atomic carbon to the C1–C2 olefinic bond yielding **i2** (mechanism 2). Both cyclic intermediates **i1** and **i2** ring open to form triplet methylbutatriene intermediates **i3′** (H$_2$CC*CCH(CH$_3$)) and **i3″** (H$_2$CCC*CH(CH$_3$)), respectively. In this scenario, it is necessary to assume that **i3′** decays nonstatistically, i.e., prior to a complete energy randomization, via atomic hydrogen loss forming 1-and 4-methylbutatrienyl radicals, i.e., CH$_3$CCCCH$_2$ and HCCCCH(CH$_3$). On the contrary, the energy randomization in **i3′** is likely to be complete and this intermediate decomposes via H atom loss to 3-vinylpropargyl, H$_2$CCCCC$_2$H$_3$. The

formation of 1-and 4-methylbutatrienyl radicals and the methyl group loss to n-C_4H_3 are very likely minor reaction channels.

The explicit verification of the carbon versus hydrogen exchange pathway together with the first identification of the 3-methylbutatrienyl radical designates a fourth synthetic route to chain C_5H_5 radicals in the reactions of atomic carbon with C_4H_6 isomers under single collision conditions, cf. Fig. 16. Experiments of atomic carbon with the 1,3-butadiene isomer demonstrated the formation of 1- and 3-vinylpropargyl radicals, $HCCCHC_2H_3$ and $H_2CCC_2H_3$, respectively, whereas the reaction with dimethylacetylene gives solely the 1-methylbutatrienyl radical. Compared to the 1,2-butadiene system, the chemical dynamics of both the 1,3-butadiene and dimethylacetylene reactions with atomic carbon are controlled by decomposing complexes long lived at all collision energies between 19.3 and 38.8 kJ mol^{-1}. The most significant difference, however, is the position of the formally inserted carbon atom within the decomposing complex, cf. Fig. 16. Considering the dimethylpropargylene intermediate, the carbon atom is located at the center-of-mass (central carbon atom; C3); the vinyl allene complex shows the former $C(^3P_j)$ at the C2 position, whereas it is found at C2 or C3 (see previous discussion) in the methylbutatriene intermediate. Therefore, the energy has to flow only via three (dimethylpropargylene) and two/three (vinylallene) bonds from the inserted carbon atom to the carbon–hydrogen bond to be cleaved. However, as found in the methylbutatriene complex, a preferential formation of the thermodynamically most stable **p4** isomer requires an energy transfer over four bonds (reactions dominated by large impact parameters). Although this argument is only qualitative, this finding suggests that the energy randomization in these decomposing methylbutatriene complexes is rather incomplete.

ACKNOWLEDGMENTS

[1] I. Hahndorf, H. Y. Lee, A. M. Mebel, S. H. Lin, Y. T. Lee, and R. I. Kaiser, J. Chem. Phys. **113**, 9622 (2000).

[2] L. C. L. Huang, H. Y. Lee, A. M. Mebel, S. H. Lin, Y. T. Lee, and R. I. Kaiser, J. Chem. Phys. **113**, 9637 (2000).

[3] H. W. Jochims, E. Rühl, H. Baumgärtel, S. Tobita, and S. Leach, Astrophys. J. **420**, 307 (1994); M. Frenklach and E. D. Feigelson, *ibid.* **341**, 372 (1998); G. von Helden, N. G. Gotts, and M. T. Bowers, Nature (London) **363**, 60 (1993); J. M. Hunter, J. L. Fye, E. J. Roskamp, and M. F. Jarrold, J. Phys. Chem. **98**, 1810 (1994).

[4] Y. T. Lee, J. D. McDonald, P. R. LeBreton, and D. R. Herschbach, Rev. Sci. Instrum. **40**, 1402 (1969).

[5] R. I. Kaiser and A. G. Suits, Rev. Sci. Instrum. **66**, 5405 (1995).

[6] G. O. Brink, **37**, 857 (1966).

[7] M. S. Weis, Ph.D. thesis, University of California, Berkeley, 1986.

[8] A. D. Becke, J. Chem. Phys. **97**, 9173 (1992).

[9] C. Lee, W. Yang, and R. G. Parr, Phys. Rev. B **37**, 785 (1988).

[10] R. Krishnan, M. Frisch, and J. A. Pople, J. Chem. Phys. **72**, 4244 (1988).

[11] G. D. Purvis and R. J. Bartlett, J. Chem. Phys. **76**, 1910 (1982).

[12] M. J. Frisch *et al.*, GAUSSIAN 94, Gaussian, Inc., Pittsburgh, 1995.

[13] MOLPRO is a package of *ab initio* programs written by H.-J. Werner and P. J. Knowles, with contributions from J. Almlöf, R. D. Amos, M. J. O. Deegan, S. T. Elbert, C. Hampel, W. Meyer, K. Peterson, R. Pitzer, A. J. Stone, P. R. Taylor, and R. Lindh.

[14] J. F. Stanton, J. Gauss, J. D. Watts, W. J. Lauderdale, and R. J. Bartlett, ACES-II, University of Florida.

[15] H. Eyring, S. H. Lin, and S. M. Lin, *Basis Chemical Kinetics* (Wiley, New York, 1980).

[16] W. B. Miller, S. A. Safron, and D. R. Herschbach, Discuss. Faraday Soc. **44**, 291 (1967).

[17] A. M. Mebel *et al.* (unpublished).

[18] *Molelucular Reaction Dynamics and Chemical Reactivity*, edited by R. D. Levine and R. B. Bernstein (Oxford University Press, New York, 1987).

[19] *Unimolecular Reaction Dynamics—Theory and Experiment*, edited by T. Baer and W. L. Hase (Oxford University Press, Oxford, 1996), Chaps. 6 and 10.

[20] J. M. Farrar and Y. T. Lee, J. Chem. Phys. **65**, 1414 (1976).